

MICROWAVE NOISE AND SMALL-SIGNAL PARAMETERS SCALING OF InP/InGaAs DHBT WITH HIGH DC CURRENT GAIN

Y. Z. Xiong, G. I. Ng, H. Wang, C. L. Law, K. Radhakrishnan and Jeffrey S. Fu

Microelectronics Center, School of Electrical and Electronics Engineering, Nanyang Technological University, Singapore 639798, Corresponding author, Tel: (65) 7904234, Fax: (65) 7933318, e-mail: eyzxiong@ntu.edu.sg

ABSTRACT

Scaling of microwave noise and small-signal parameters of InP-based Double Heterojunction Bipolar Transistors (DHBTs) with high DC current gain is presented. Three different sizes of InP/InGaAs DHBT are investigated in this work. Because of the low surface and intrinsic recombination of the InP-based DHBT with high current gain, the extrinsic parasitic effect of the device can be neglected. Thus, the microwave parameters of large size InP DHBT can be obtained by scaling the parameters of the smaller emitter size device. Good agreement was obtained between the measured and the calculated results. This scaling technique is very useful for the design of high frequency circuits using InP-based HBTs.

1. INTRODUCTION

InP/InGaAs Heterojunction Bipolar Transistors (HBTs) have exhibited excellent microwave and noise performance and are very attractive for many applications such as high-speed digital circuits, oscillators and low noise amplifiers [1], [2], [3]. The high performances are due to the excellent electron transport properties of InGaAs and the low surface recombination velocity [4]. In GaAs HBT, many researchers have used emitter-ledge to reduce the surface recombination current, thereby increasing the current gain to improve the HBT performances [5]. By using an ultra-thin AlGaAs emitter layer for the extrinsic base surface passivation, the current gain of GaAs HBTs with small size emitter can be maintained to that of large-size emitter devices [6]. As a result, the impact of the device geometric structure and the emitter size on the device performance is significantly reduced. Although the noise scalability of SiGe bipolar transistor was reported in [7], the relationship of noise parameters with emitter-size is not given accurately, and the operating frequency is only 1.6 GHz. Since InP Double Heterojunction Bipolar Transistors (DHBTs) possess

inherent low surface recombination velocity, the emitter-size does not have a big effect on the current gain. As a result, an InP-DHBT of larger size emitter can be viewed as consisting of many smaller emitter sub-cells of identical size connected in parallel [8], [9]. Once the microwave parameters of the sub-cells are known, the parameters of the large-size DHBT can be obtained using the technique developed in this study. The impact of the external base-collector capacitor on the scalability of InP/InGaAs DHBTs is also addressed in this work. The good agreement obtained between the measured and the fitted results validate the technique, which is helpful for the design of high frequency circuits using InP-based HBTs.

2. SCALING THEORY

Fig.1 shows the top view of a large-size emitter DHBT. The large-size emitter DHBT can be viewed as consisting of two identical sub-cells with smaller emitter strip width connected in parallel. Assuming that one of the two sub-cells has Y-parameters $[Y_1]$ and noise parameters $[NF_{MIN}^1]$, $[R_N^1]$ and $[Y_{OPT}^1]$, and the other sub-cell has Y-parameters $[Y_2]$ and noise parameters $[NF_{MIN}^2]$, $[R_N^2]$ and $[Y_{OPT}^2]$, and that the two sub-cells are identical, then the noise parameters of the large-size emitter DHBT can be expressed as:

$$[Y] = [Y_1] + [Y_2] \quad (1)$$

$$NF_{MIN} = NF_{MIN}^1 = NF_{MIN}^2 \quad (2) \quad R_N = \frac{R_N^1}{2} = \frac{R_N^2}{2} \quad (3)$$

$$G_{OPT} = 2G_{OPT}^1 = 2G_{OPT}^2 \quad (4) \quad B_{OPT} = 2B_{OPT}^1 = 2B_{OPT}^2 \quad (5)$$

where the NF_{MIN} is the minimum noise figure of the large-size emitter DHBT, and NF_{MIN}^1 and NF_{MIN}^2 are the minimum noise figures of the sub-cells. R_N , R_N^1 and R_N^2 are the noise resistances, G_{OPT} , G_{OPT}^1 , and G_{OPT}^2 and

B_{OPT} , B_{OPT}^1 , and B_{OPT}^2 are the real and imaginary parts of the optimum input admittances for the large-size emitter and sub-cells, respectively.

Using the same analogy, the noise parameters and Y-parameters of the large-size emitter DHBT consisting of n identical sub-cells can be expressed as follows:

$$[Y] = n[Y^{sub}] \quad (6)$$

$$NF_{MIN} = NF_{MIN}^{sub} \quad (7) \quad R_N = \frac{R_N^{sub}}{n} \quad (8)$$

$$G_{OPT} = nG_{OPT}^{sub} \quad (9) \quad B_{OPT} = nB_{OPT}^{sub} \quad (10)$$

where $[Y]$ and $[Y^{sub}]$ are the Y-parameters of the large-size emitter DHBT and the sub-cells, respectively; NF_{MIN} and NF_{MIN}^{sub} are the minimum noise figures, R_N and R_N^{sub} are the noise resistances, G_{OPT} , G_{OPT}^{sub} and B_{OPT} , B_{OPT}^{sub} are the real and imaginary parts of the optimum input admittances of the large-size emitter DHBT and the sub-cells, respectively.

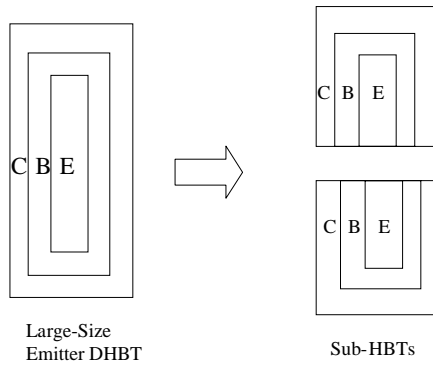


Fig. 1 The top view of a large-size emitter DHBT viewed as two sub-small size emitter DHBTs.

3. EXPERIMENTS AND VERIFICATION

In order to verify the microwave parameter scalability, lattice-matched InP/InGaAs DHBTs were used. Details of the layer structures and the fabrication process have been reported in [10]. The three InP/InGaAs common-emitter DHBTs with emitter area of $5 \times 20 \mu\text{m}^2$, $5 \times 10 \mu\text{m}^2$ and $5 \times 5 \mu\text{m}^2$, respectively, were investigated in this work. Fig. 2 shows a typical Gummel plot for $5 \times 5 \mu\text{m}^2$ of InP-DHBT. These devices exhibited an average extrinsic peak current gain of 180 and are almost constant over the entire operating range. The ideality factors of the collector and the base currents for the emitter area of $5 \times 5 \mu\text{m}^2$ are ~ 1.1 and ~ 1.2 , respectively.

Microwave parameters were measured on-wafer over the frequency range of 2 to 20 GHz using an ATN-NP5

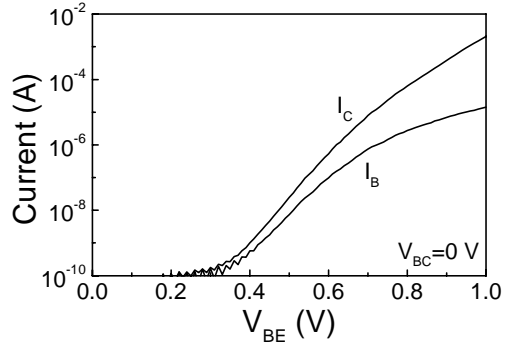


Fig. 2 A typical Gummel plot for $5 \times 5 \mu\text{m}^2$ of InP DHBT.

microwave noise measurement system and Cascade microwave probes. In order to verify the device scalability, the noise parameters and S-parameters for $5 \times 20 \mu\text{m}^2$, $5 \times 10 \mu\text{m}^2$ and $5 \times 5 \mu\text{m}^2$ devices at the same collector current density and collector-emitter voltage were also measured. Fig. 3 shows the fitted and measured S-parameters for the $5 \times 20 \mu\text{m}^2$ device. Fitted Y-parameters for $5 \times 20 \mu\text{m}^2$ can be calculated using Equation (6) from the measured Y-parameters of $5 \times 10 \mu\text{m}^2$ device. Good agreements were obtained between the fitted and the measured S-parameter. However, the errors increased if the S-parameters of the $5 \times 5 \mu\text{m}^2$ device were used to fit the S-parameters of the $5 \times 20 \mu\text{m}^2$ device. To explain the observed errors, different ratios between the internal base-collector and external base-collector capacitors due to the different DHBT geometry and layout for the three devices were extracted. The ratios between the emitter-base area and the base-collector area of the $5 \times 20 \mu\text{m}^2$, $5 \times 10 \mu\text{m}^2$ and $5 \times 5 \mu\text{m}^2$ devices are 100/321, 50/181 and 25/111, respectively. The extracted internal/external base-collector capacitors of $5 \times 20 \mu\text{m}^2$, $5 \times 10 \mu\text{m}^2$ and $5 \times 5 \mu\text{m}^2$ devices at the same collector current density $J_C = 40 \text{ A/mm}^2$ and collector-emitter voltage $V_{CE} = 1.5 \text{ V}$ are 46.2ff/132ff, 24.3ff/78.5ff and 13.2ff/55.5ff, respectively. From the above results, it is shown that the internal base-collector capacitors are almost scalable, but the external base-collector capacitors are not scalable as a result of the non-scalable base-collector area.

To analyze the effect of external base-collector capacitor on the scaling of Y-parameters, the relative error values are used [11]. The fitting errors on the Y-parameters caused by non-scalable external base collector capacitor are shown in Table I. It is shown that as the ratios between the emitter-base area and the base-collector area increase, the errors for the fitted Y-parameters increase, especially for Y_{12} . In order to further illustrate the effect of external base-collector on the Y-

parameters, the small-signal equivalent circuit simulation of the $5 \times 20 \mu\text{m}^2$ device was done using the base-collector capacitor value of four times the $5 \times 5 \mu\text{m}^2$ device or two times the $5 \times 10 \mu\text{m}^2$ device instead of using directly the external base-collector capacitor value of the $5 \times 20 \mu\text{m}^2$ device. HP-ADS was used for the simulation of the equivalent circuit. The agreement between the simulated Y-parameters and the fitted Y-parameters using the Y-parameters of $5 \times 10 \mu\text{m}^2$ and $5 \times 5 \mu\text{m}^2$ devices is good when Equation (6) was used. This demonstrates that the fitting errors for Y-parameters in Table I are caused by the external base-collector capacitor. After correcting the external base-collector capacitor value by using four times the capacitor value of $5 \times 5 \mu\text{m}^2$ device or two times the capacitor value of $5 \times 10 \mu\text{m}^2$ device, all the fitted errors are found to be less than 1%.

The measured and the fitted NF_{MIN} of $5 \times 20 \mu\text{m}^2$, $5 \times 10 \mu\text{m}^2$ and $5 \times 5 \mu\text{m}^2$ devices at the same collector current density $J_C = 80 \text{ A/mm}^2$ and collector-emitter voltage $V_{CE} = 1.5 \text{ V}$ are shown in Fig. 4. Although the base-collector capacitors are different, the agreement between the measured noise figures at the lower frequencies is good for the $5 \times 20 \mu\text{m}^2$, $5 \times 10 \mu\text{m}^2$ and $5 \times 5 \mu\text{m}^2$ devices thus verifying the validity of Equation (7). For $5 \times 10 \mu\text{m}^2$ and $5 \times 5 \mu\text{m}^2$ devices, the measured minimum noise figure is slightly lower than the large devices at higher frequencies. This may be due to the fact that the base-collector capacitors act as negative feedbacks thus reducing the minimum noise figure, especially at higher frequencies. Fig.5 shows the measured and the fitted equivalent noise resistance versus frequency. The measured noise resistance of $5 \times 20 \mu\text{m}^2$ device is almost equivalent to one-fourth of the measured noise resistance of $5 \times 5 \mu\text{m}^2$ device and half of the $5 \times 10 \mu\text{m}^2$ device at low frequency range. However, at

Table I Fitting percentage errors of the Y-parameters and noise parameters between measured and fitted.

	$J_C = 40 \text{ A/mm}^2$			$J_C = 80 \text{ A/mm}^2$		
	5x10 fit to 5x20	5x5 fit to 5x10	5x5 fit to 5x20	5x10 fit to 5x20	5x5 fit to 5x10	5x5 fit to 5x20
A_{EB}/A_{BC}	5.3	14.0	47.9	5.3	14.0	47.9
Y_{11}	1.7	5.4	15.4	2.0	6.2	17.8
Y_{12}	2.9	20.0	48.5	3.1	21.5	52.1
Y_{21}	2.2	3.1	12.1	1.6	3.2	14.4
Y_{22}	1.2	7.0	16.1	1.2	6.3	14.4
R_N	1.8	6.8	12.7	2.2	5.3	11.7
NF_{MIN}	0.54	7.1	6.3	0.2	7.3	5.5
Total	2.2	13.5	27.7	2.2	12.8	27.7

higher frequencies, the errors increase. If, instead of the external base-collector capacitor of $5 \times 20 \mu\text{m}^2$, one uses four times of the external base-collector capacitor value of the $5 \times 5 \mu\text{m}^2$ ($4 \times 55.5 \text{ ff}$) device for simulation, the

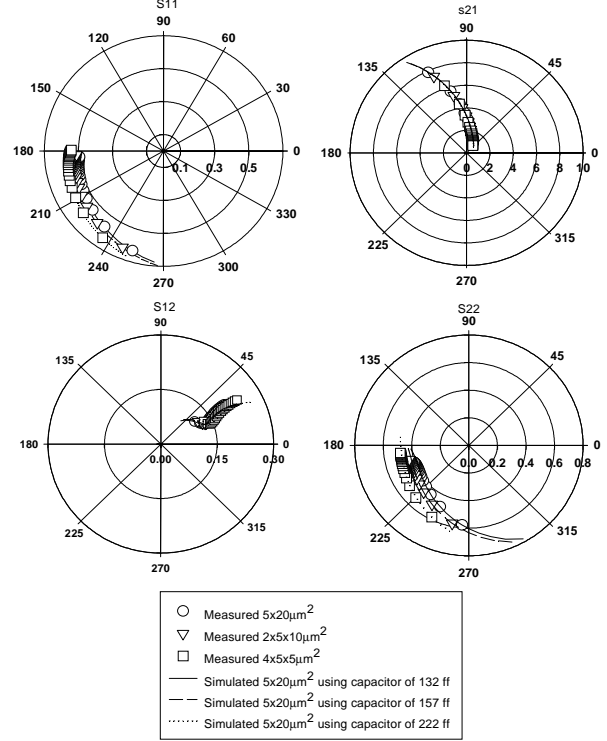


Fig.3 Comparison of measured or fitted and simulated. $S11$, $S21$, $S12$ and $S22$ from 2-20GHz, $V_{CE} = 1.5 \text{ V}$ and $J_C = 40 \text{ A/mm}^2$.

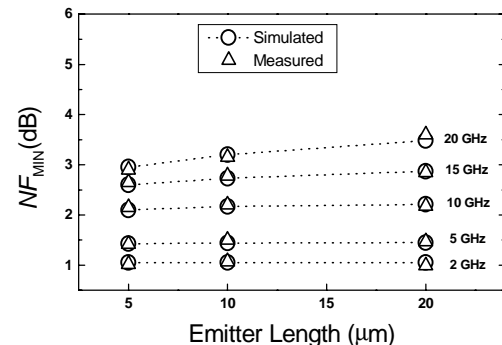


Fig.4 Comparison of the measured and simulated minimum noise figures (NF_{MIN}). Measured minimum noise figures (Δ) for the $5 \times 5 \mu\text{m}^2$, $5 \times 10 \mu\text{m}^2$ and $5 \times 20 \mu\text{m}^2$ at different frequencies. And simulated minimum noise figures (\circ) for $5 \times 20 \mu\text{m}^2$ instead of external base-collector capacitor (132 ff) by four times or two times of the $5 \times 5 \mu\text{m}^2$ ($5 \times 55.5 \text{ ff}$) or $5 \times 10 \mu\text{m}^2$ ($2 \times 78.5 \text{ ff}$).

results show that the minimum noise figures agree well with the measured results of the $5 \times 20 \mu\text{m}^2$ device at low frequency. The simulated noise figures are identical to the measured values of $5 \times 5 \mu\text{m}^2$ device. The experimental and simulated results show that the optimum source admittances are also scalable.

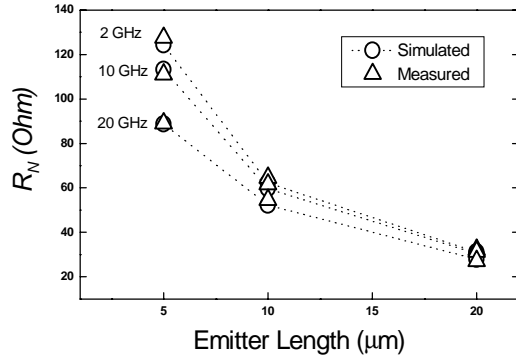


Fig.5 Comparison of the measured and simulated R_N at different frequencies. Measured R_N (Δ) for the $5 \times 5 \mu\text{m}^2$, $5 \times 10 \mu\text{m}^2$ and $5 \times 20 \mu\text{m}^2$. Simulated (\circ) for $5 \times 20 \mu\text{m}^2$ instead of external base-collector capacitor (132 fF) by four times or two times of the $5 \times 5 \mu\text{m}^2$ (4x55.5 fF) or $5 \times 10 \mu\text{m}^2$ (2x78.5 fF); at emitter length of $5 \mu\text{m}$, R_N is four times of simulated with 4x55.5 fF; at emitter length of $10 \mu\text{m}$, the R_N is two times of simulated with 2x78.5 fF.

4. CONCLUSION

The scalability of microwave noise and small-signal parameters of InP double heterojunction bipolar transistor is investigated in this work. Our results show that by taking the external base-collector capacitor into consideration, good scalability can be obtained between large and small devices. A set of equations has been proposed to relate the small-signal parameters and noise parameters of the large and small size devices. Good agreement between the measured and the simulated results was obtained suggesting the validity of our approach. This scalability technique will be useful for the design of high frequency circuits using InP-based HBTs.

ACKNOWLEDGMENT

The authors wish to thank Prof. S. F. Yoon, Mr. H.Q. Zheng, and Mr. C. L.Tan, for their helpful discussions. This work is supported by the grant under the National Science and Technology Board of Singapore and the Ministry of Education funded project (JT MLC 2/98).

REFERENCES

- [1] K.W. Kobayashi; A.K. Oki; L.T. Tran; J.C. Cowles; A. Gutierrez-Aitken; F. Yamada; T.R. Block; and D.C. Streit, "A 108-GHz InP-HBT monolithic push-push VCO with low phase noise and wide tuning bandwidth," *IEEE Journal of Solid-State Circuits*, vol.34, pp.1225-1232, Sept. 1999.
- [2] K. W. Kobayashi, J. Cowles, L. T. Tran, A. Gutierrez-Aitken, T. R. Block, A. K. Oki, and D. C. Streit, "A 50-MHz-55-GHz multidecade InP-based HBT distributed amplifier," *IEEE Microwave and Guided Wave Lett.*, vol.7, pp.353 -355, 1997.
- [3] M. Rodwell, Q. Lee, D. Mensa, J. Guthrie, Y. Betser, S. C. Martin, R. P. Smith, S. Jaganathan, T. Mathew, P. Krishnan, C. Serhan, and S. Long, "Transferred-substrate heterojunction bipolar transistor integrated circuit technology," in Proc. 11th Int. Conf. Indium Phosphide and Related Materials(IPRM), pp.169 -174, 1999.
- [4] R. N. Nottenburg, Y.K.Chen, M.B. Panish, R.Hamm, and D.A.Humphery, "High gain submicrometer InGaAs/InP heterojunction bipolar transistors" *IEEE Electron Device Lett.*, vol. 9, pp.524-526, 1988.
- [5] D. Costa, M. N. Tutt, A. Khatibzadeh, and D. Pavlidis, "Tradeoff between 1/f noise and microwave performance in AlGaAs/GaAs heterojunction bipolar transistors," *IEEE Electron Devices*, vol.41, No.8 pp.1347-1350, Aug. 1994.
- [6] R. J. Malik, L. M. Lunardi, R. W. Ryan, S. C. Shunk, and M. D. Feuer, "Sub-micron scaling of AlGaAs/GaAs self-aligned thin emitter heterojunction bipolar transistors (sate-HBT) with current gain independent of emitter area," *IEE Electronics lett.*, vol.25, No. 17, pp.1175-1177, Aug.1989.
- [7] S. P Voinigescu, M. C. Maliepaard, J. L. Showell, G. E. Babcock, D. Marchesan, M. Schroter; P. Schvan, and D. L. Harame, "A scalable high-frequency noise model for bipolar transistors with application to optimal transistor sizing for low-noise amplifier design," *IEEE Journal of Solid-State Circuits*, vol. 32, pp.1430, Sept. 1997.
- [8] W. Liu; S. Nelson; D.G. Hill; and A. Khatibzadeh, "Current gain collapse in microwave multifinger heterojunction bipolar transistors operated at very high power densities" *IEEE Transactions on Electron Devices*, vol.40, pp.1917 - 1927, Nov. 1993.
- [9] R. Hajji and F.M. Ghannouchi, "Small-signal distributed model for GaAs HBT's and S-parameter prediction at millimeter-wave frequencies," *IEEE Transactions on Electron Devices*, vol.44, pp.723 -732, May 1997.
- [10] Hong Wang, Geok Ing Ng, Haiqun Zheng, Yong Zhong Xiong, Lye Heng Chua, Kaihua Yuan, K. Radhakrishnan, and Soon Fatt Yoon, "Demonstration of Aluminum-free Metamorphic InP/In_{0.53}Ga_{0.47}As/InP Double Heterojunction Bipolar Transistors on GaAs Substrates," *IEEE Electron Device Letter*, vol. 21, no.9, pp.379-381, September, 2000.
- [11] Bin Li, S. Prasad, L.W. Yang, and S. C. Wang, "A semi-analytical parameter-extraction procedure for HBT equivalent circuit," *IEEE Transaction on Microwave and Theory and Techniques*, vol.46, No.10, pp.1427-1435, 1998.